Experimental study of overexpanded co-flowing jets

H. Sharma, A. Vashishtha, E. Rathakrishnan
Department of Aerospace Engineering, Indian Institute of Technology
Kanpur, India.

P. Lovaraju
Department of Mechanical Engineering, K.L. College of Engineering
Vijayawada, AP, India

ABSTRACT

An experimental investigation was carried out to find the effect of an annular co-flow jet on the primary supersonic jet from Mach 2 nozzle at different levels of overexpansion. In this study, a convergent-divergent circular nozzle of exit Mach number 2, surrounded by an annular convergent circular nozzle with an annular gap of 4·4mm was used. Nozzle pressure ratios (NPRs) 3, 4, 5, 6, 7 are investigated for overexpanded states of the primary jet and NPR 8 is investigated for almost correctly expanded state. The centreline pressure distributions were taken at all NPRs for both with and without co-flow case, to investigate the supersonic core extent and mixing activity in the jet field. In the radial direction pitot pressure at different axial locations at all NPRs for both the cases are measured to find the jet development and shadowgraph visualisation of jet structure was done to visualise the shock structure in near-field. It is found that the co-flow acts as mixing inhibitor at all levels of overexpansion for Mach 2 nozzle.

NOMENCLATURE

CPD	centreline pitot pressure distribution
D	primary nozzle exit diameter
M_e	primary nozzle exit Mach number
NPR	primary nozzle pressure ratio (P_0/P_a)
P_a	atmospheric or ambient pressure
P_e	static pressure at primary nozzle exit
P_e/P_a	expansion level at primary nozzle exit
P_0	stagnation chamber pressure
P_t	pitot pressure
R	radial direction (primary jet)
X	primary jet axis

1.0 INTRODUCTION

Co-flowing jets are inherently present in all the exhaust systems of moving vehicles. When the flow exiting the nozzle encounters a stationary atmosphere, it is termed submerged jets. The mixing and propagation characteristics of submerged jets are well documented. When the flow encounters a moving boundary as in the case of moving vehicles, the entrainment characteristics are greatly influenced by the co-flow. Co-flowing jets are emerging as an interesting field of jet control for academic and industrial research. Co-flow jets find application in a variety of practical devices, such as aircraft engine exhaust, fuel injectors and so on. A control over the moving jet boundary surrounding the primary jet has several industrial applications such as exhaust disposal of industrial chimneys and automobile engines. Earlier works on co-flow jets were motivated mainly by the applications in combustion and aircraft propulsion. Also, co-flow jets are used to provide the mixing between the fuel and oxidizer in the gas turbine combustors. The hot supersonic jets exhausting from the high-speed civil transport engines are powerful noise generators especially during take-off, which is one of the major technical hurdles facing the future supersonic transport. They create noise levels which are environmentally unacceptable. The noise emitted from these engines is objectionable as per the noise regulations. It has been found that the near and far-field of supersonic jets are much noisier than subsonic jets, due to the intense Mach wave radiation[1,2]. Mach wave elimination is achieved by surrounding the supersonic jet with an annular stream at prescribed velocity and temperature. Marco Debiasi and Dimitri Papamoschou[3] studied the effect of an annular co-flow on noise characteristics of perfectly and imperfectly expanded co-axial jets. It has been reported that the co-flow suppresses Mach wave emission most effectively in jets with fully expanded velocity. In co-axial flows the secondary flow reduces the growth rate of the primary shear layer and

Paper No. 3271. Manuscript received 2 January 2008, revised 18 March 2008, accepted 6 May 2008.

https://doi.org/10.1017/S0001924000002499 Published online by Cambridge University Press

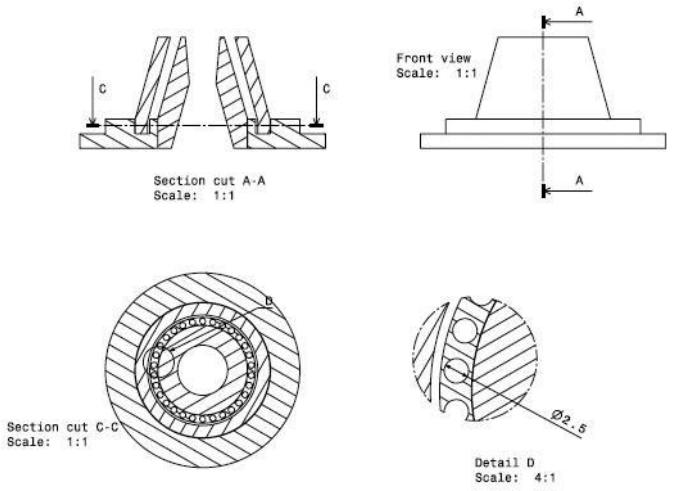


Figure 1(a). Schematic diagram of nozzle assembly.

elongates the primary potential core and the supersonic region of the jet[4]. Sukumar *et al*[5] reported that core length of sonic underexpanded primary jet is increased by co-flow at all levels of underexpansion. The level of expansion plays a dominant role in elongating the primary jet core length. The co-flow retards the mixing of the primary jet causing the potential core elongation[6].

Modern jet research focuses on the effect of co-flow on a primary jet to modify the mixing characteristics, thereby enhancing or inhibiting the mass entrainment of the primary jet. The limited information available in open literature focuses on co-flow effect on few specific cases of primary jet. Also, the shear layer physics governing the process which modifies the core of supersonic primary jets are hardly looked into. Keeping this in view, the present study aims at understanding the flow physics behind the behavior of overexpanded and correctly expanded Mach 2 primary jet in the presence of a co-flow.

2.0 EXPERIMENTAL DETAILS

The experiments were carried out in an open jet facility at the High-Speed Aerodynamics Laboratory, Indian Institute of Technology Kanpur. The co-flow model studied consists of a convergent-divergent primary nozzle surrounded by a convergent nozzle. The primary nozzle exit diameter is 14·2mm and the lip thickness at the exit of the primary nozzle is 1·7mm. Outer nozzle exit diameter is 25·6mm and annular gap between the two nozzles is 4mm. Schematic and photographic views of the experimental model are shown in Fig. 1. Experiments were carried out using the primary nozzle alone (without co-flow) and with both primary and surrounding nozzle (with co-flow). The nozzle pressure ratio (NPR) is defined as the ratio of settling chamber pressure (P_0) to the ambient atmospheric pressure (P_a) to which the jets are discharged. This is the conventional way of defining NPR for submerged jets. But, for co-flow jets this NPR should be taken only as an indication of the stagnation pressure at the nozzle inlet. This is because the environment to which the primary jet is discharged will be equal to P_a only when the co-flow nozzle exit Mach number is subsonic or correctly expanded sonic. When the co-flow jet is underexpanded sonic jet, the surrounding pressure to which the primary jet is discharged is higher than P_a. Therefore, the effective value of nozzle pressure ratio will be the ratio of P_0 and the pressure prevailing in the co-flow jet. But, in an underexpanded co-flow the static pressure is not a constant due to wave domination. Therefore, specifying the nozzle pressure ratio is not possible. Hence the NPR in the present case should be taken as the dimensionless stagnation pressure in the settling chamber which runs both the primary and co-flow nozzles.

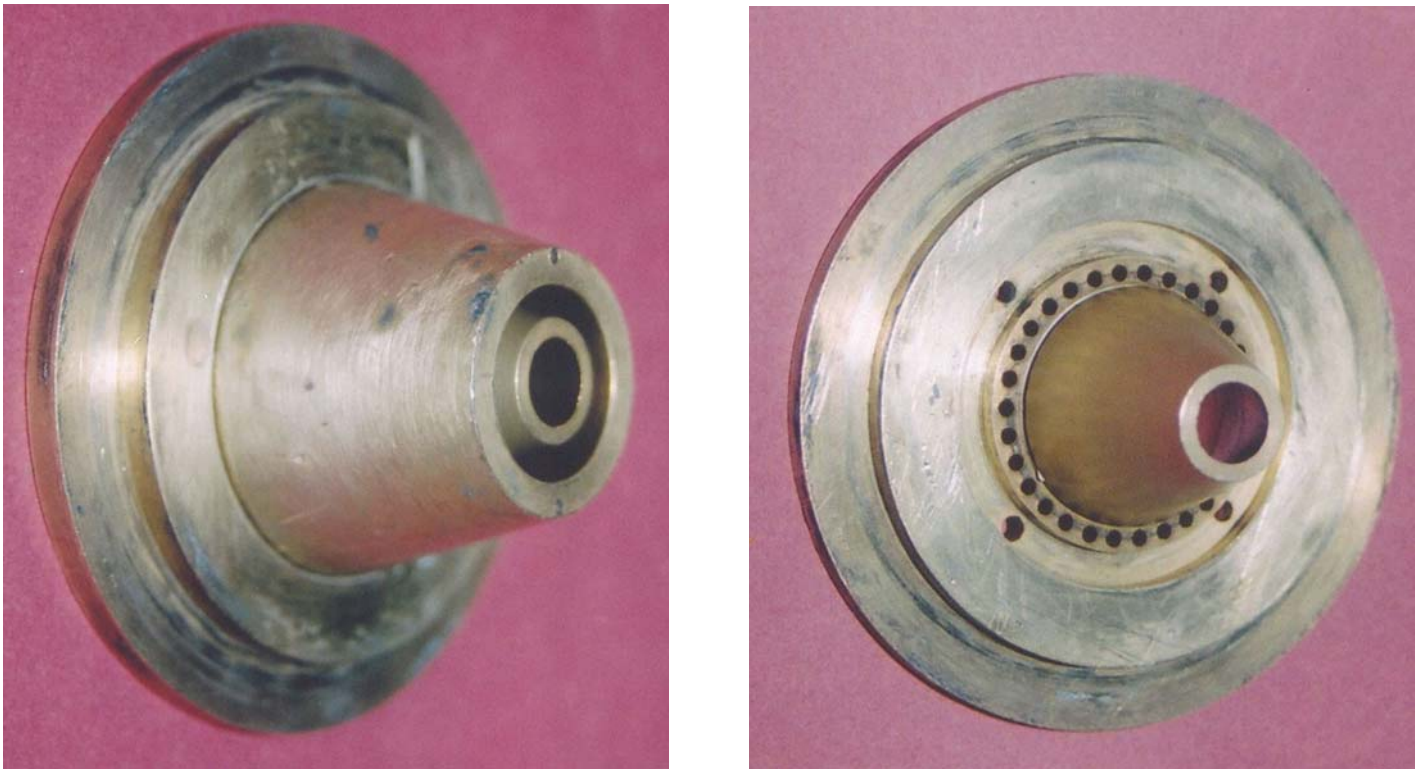
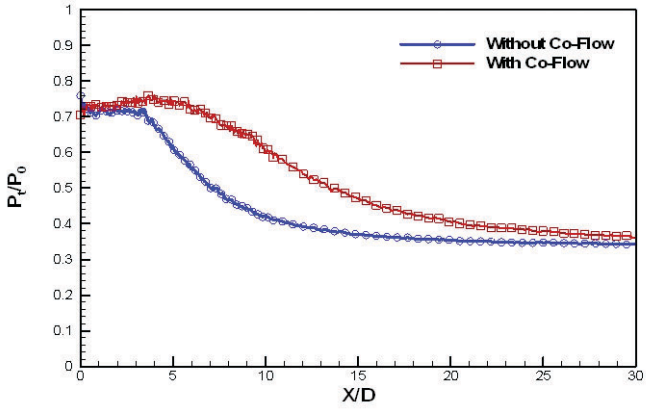
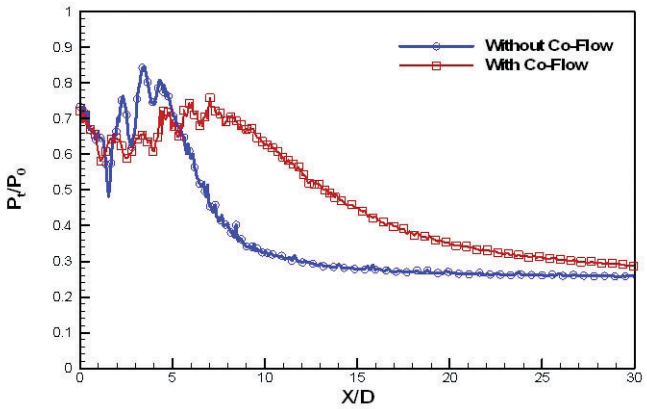


Figure 1(b). Photographic view of co-flowing nozzle.

https://doi.org/10.1017/S0001924000002499 Published online by Cambridge University Press



2(a) CPD Profile at NPR 3



2(b) CPD Profile at NPR 4

Figure 2 (a-b). Centreline pitot pressure distribution.

Pressure measurements were made using a pitot probe of 0·4mm inner diameter and 0·6mm outer diameter mounted on a traverse mechanism. The pitot pressure and the stagnation chamber pressure were measured with a 9016 model pressure transducer. Application software LabVIEW was used to interface transducer and the computer. The pitot pressures were measured along the jet axis up to X/D = 30. The radial pitot pressure measurements were taken at 14 different axial locations. Nozzle pressure ratios (NPR) chosen were 3-8, in steps of 1. In this investigation both the primary and co-flow nozzles were run by the same settling chamber. Thus, the stagnation pressure P_0 at the entrance of primary and co-flow nozzles is the same. To understand the shock structure, shadowgraph technique was employed. Shadowgraph pictures were taken for both without and with co-flow cases.

2.1 Data accuracy

The possible sources of error of the present investigation are due to

- The linear movement of traverse along X, Y and Z directions.
- The settling chamber stagnation pressure measurement.
- The error in the measurement of total pressure in the jet field.
- The possible inaccuracies in nozzle dimensions.

The room temperature was almost constant with maximum variation of ±0·5°C during one experimental run. The stagnation pressure was maintained manually with an accuracy of ± 0·1% through the application software developed in Lab VIEW. Finally, although great care was taken in pitot pressure measurements, the possibility of some inaccuracy in these measurements, in a highly turbulent and three-dimensional flow field as in the present case cannot be ruled out. But it may be justifiably assumed that, this slight inaccuracy may not affect the results significantly as the results are primarily of comparative nature.

3.0 RESULTS AND DISCUSSION

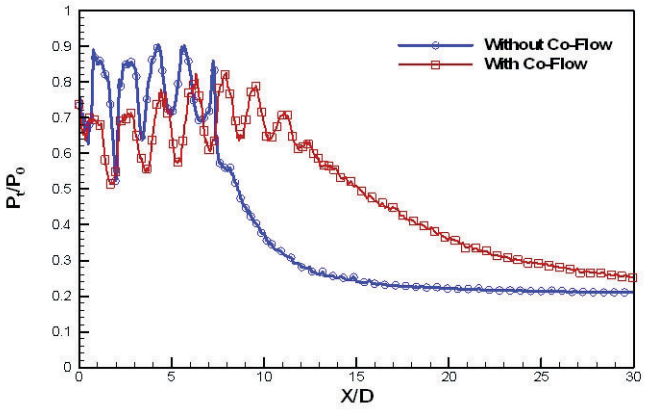
To gain an insight into the physics of the effect of a co-flow in the overexpansion regime, NPR 3-7 were chosen for the study. The overexpansion level is the ratio of nozzle exit pressure to the ambient pressure. The overexpansion level (P_e/P_a) for Mach 2 convergent-divergent nozzle operated at NPRs 3, 4, 5, 6 and 7 are 0·38, 0·51, 0·64, 0·77 and 0·89, respectively. In an overexpanded jet, the nozzle exit pressure (P_e) is less than the ambient pressure (P_a). Here again P_a is used to non-dimensionalise the exit pressure (P_e). The pressure in the field of co-flow surrounding the primary jet is equal to P_a when the co-flow is subsonic. But, when the co-flow is underexpanded, the pressure in the field varies from point to point. Therefore, for such a case there is no fixed static pressure available for non-dimensionalising the exit pressure P_e. Hence the pressure of the ambient atmosphere is used as the representative back pressure for the underexpanded co-flow also. Even though P_a is not the actual back pressure, it may be taken as good enough for qualitative characterization of primary jet behaviour. For overexpanded operation, the pressure imbalance at the nozzle exit causes an oblique shock to form at the nozzle exit plane. To reach equilibrium with the ambient pressure the flow undergoes compression through the oblique shock wave at the exit plane. This oblique shock wave is reflected as expansion waves at the jet boundary downstream of nozzle exit and the whole process is repeated till the local static pressure comes to equilibrium with ambient pressure.

3.1 Centreline pitot pressure distribution (CPD)

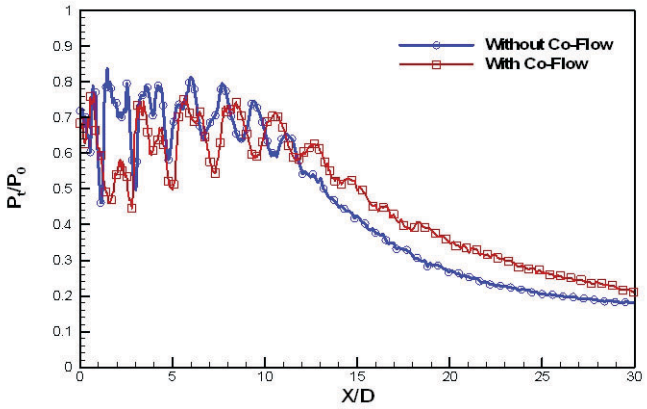
The supersonic core is the axial extent up to which waves (compression and expansion waves) prevail[7]. The measured pitot pressure (P_t) is non-dimensionalized with the stagnation pressure (P_0) and plotted against the axial distance (X) non-dimensionalized with the primary nozzle exit diameter (D). The centreline pressure distributions of the jet operated at NPRs 3, 4, 5, 6, 7 and 8, with and without co-flow are shown in Fig. 2. In the supersonic regime of the flow, the measured pitot pressure (P_t) corresponds to the total pressure behind the standing bow shock in front of the probe nose. In the subsonic regime of the flow, the pressure measured by the pitot probe is the local stagnation pressure. The oscillations in the centreline pressure distribution plots imply the presence of shock-cells in the jet field. Due to the probe interference with the shock structure, there could be some measurement error and hence results are only qualitative in nature. But the measured data is good enough to capture the vital details such as the supersonic core length, length of shock cells and the strength of shocks[7].

For NPR 3 (Fig. 2(a)), the supersonic core prevails up to X/D = 3·8 for without co-flow and X/D = 6·2 in the presence of co-flow. Similarly, for NPR 4, the axial extent of the pitot pressure oscillations extends up to X/D = 4·6 and 9·4 for without co-flow and with co-flow, respectively. An increase in the core length of about 63% at NPR 3 and 104% at NPR 4 (Fig. 2(b)), is caused by the co-flow. At NPR 3, there is no significant pitot pressure oscillation in the jet field. It means that the waves prevailing in the jet field are weak. On

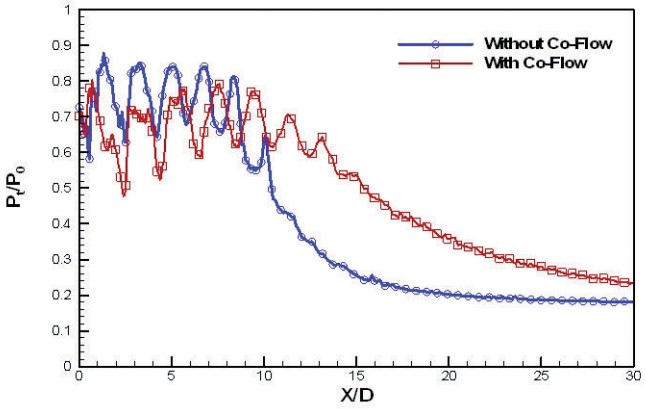
https://doi.org/10.1017/S0001924000002499 Published online by Cambridge University Press



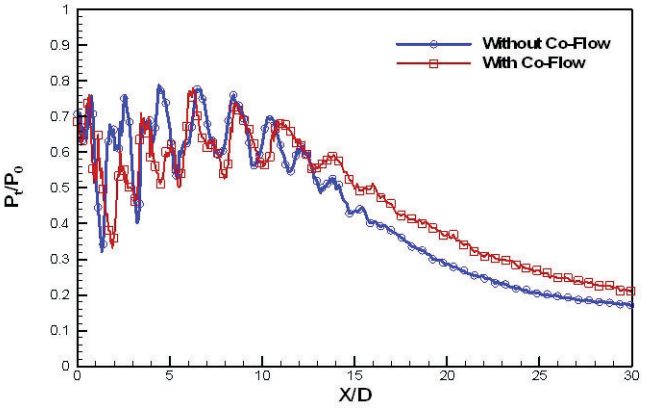
2(c) CPD Profile at NPR 5



2(e) CPD profile at NPR 7



2(d) CPD profile at NPR 6



2(f) CPD profile at NPR 8

Figure 2 (c-f). Centreline pitot pressure distribution.

the contrary, as the overexpansion level is decreased, at NPR 4, shock cells are evident from the pitot pressure oscillations for both with and without co-flow. For the plain jet (without co-flow) at NPR 4, a steep drop in the pitot pressure is seen at about $X/D = 2$, which indicates the presence of a strong shock, probably a small Mach disc (which is seen clearly from the shadowgraph picture of the plain jet at NPR 4, Fig. 5(c)). In the presence of co-flow, the first minima in centreline pitot pressure occurs upstream of that for without co-flow. This is because of Mach disc formation and the accompanying shortening of the first shock cell upon the introduction of co-flow. The number of shock cells has increased with co-flow but the strength decreased considerably as seen from the amplitude of the pitot pressure oscillations. Also, the characteristic decay in the presence of co-flow is very shallow compared to without co-flow case. Due to the presence of a moving boundary, a comparatively lesser velocity differential between the two layers. This gives rise to the formation of small vortices at the main jet boundary, eventually being carried away downstream, by the large momentum of the jet. These small vortices have higher momentum in the axial direction and have a longer life compared to the vortices that are formed between the quiet ambient and the plain jet (without co-flow case). Hence, due to the presence of a moving boundary imparting a considerably reduced shear to the inner jet boundary, the flow can be turned quickly inwards, thereby shortening the first shock cell and making the intercepting shocks to become stronger. As can be seen from the centreline pitot pressure distribution (CPD) plots, at all the overexpanded operating conditions the characteristic decay is very steep for the plain jet. When the co-flow is introduced, pitot pressure decay becomes gradual enabling the jet to prevail over longer distances in far-field. For NPR 5 (Fig. 2(c)), the extent of supersonic core is 7·2D and 12·2D, for without and with co-flow cases, respectively. For NPR 6 (Fig. 2(d)) the supersonic core length is up to $X/D = 10·3$ for without co-flow and up to $X/D = 13·8$ for with co-flow. For NPR 5 and 6, core length is increased by 69% and 34 %, respectively. As the NPR increases, the overexpansion level is decreased. This decrease reduces the possibility of Mach disc formation in the jet core. Shadowgraph pictures (for NPR 5, Figs 5(e) and 5(f)) for plain jet clearly reveal the shock cross-over point at the jet centreline. From the CPD plots, a sharp decay is seen in pitot pressure, indicating the probe passing through the shock cross-over point. The strength of the shocks for plain jet is higher compared to with co-flow case. Lower amplitudes of the pitot pressure oscillations for co-flow result in an increase in the number of shock cells, implying a delay in the mixing activity. Shadowgraph picture (Fig. 5(f)) for with co-flow case indicates the presence of a small Mach disk in the first shock cell. In the presence of co-flow the amplitude decreases with axial distance. This is evident from the centreline plot (Fig. 2(c)) seen from the sharp drop in the pitot pressure at about $X/D = 2$ after a small rise in the pitot pressure. As it is evident from the CPD plot at NPR 6 (Fig. 2(d)), the amplitudes of pitot pressure are not much different from those for without co-flow. The crest points for co-flow case are lower than those of no co-flow, throughout the supersonic core region. In the presence of co-flow the amplitude decreases with axial distance. But when there is no co-flow, the

https://doi.org/10.1017/S0001924000002499 Published online by Cambridge University Press

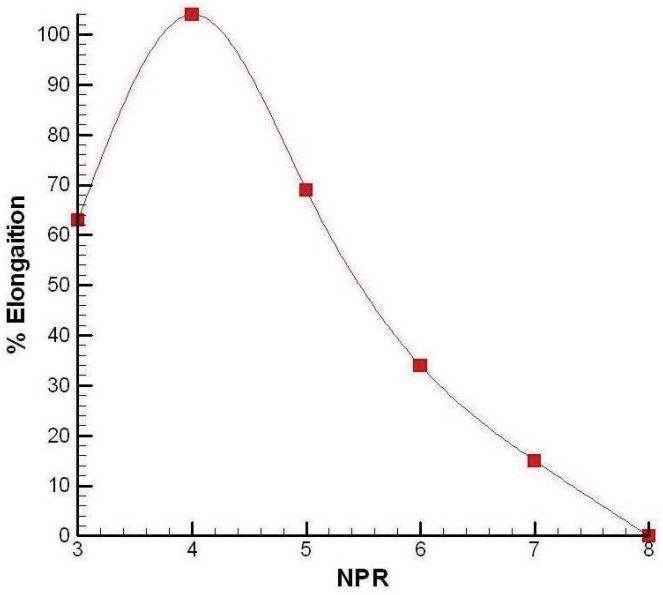


Figure 3. Percentage elongation in supersonic core.

amplitude decreases very gradually through the supersonic core.

The axial extent of the pitot pressure oscillations is 11·1*D* and 12·8*D* for without and with co-flow at NPR 7, respectively (Fig. 2(e)). This corresponds to an elongation of 15% in the supersonic core at NPR 7. Number of shock-cells is almost closer for both the cases, i.e. 9 for without co-flow and 10 for with co-flow. In this case also, the pitot pressure oscillates with almost the same amplitude for both the cases. The characteristic decay is gradual for the plain jet too at NPR 7. At NPR 8, the core-length is almost the same (X = 14D), for both with and without co-flow. For Mach 2 jet isentropic correct expansion NPR is 7·82. Therefore, NPR 8 may be treated as correctly expanded condition for the actual jet. In this case, the numbers of shock cells are the same in both the cases; also the characteristic decay indicates the same slope in both the cases. But, in the fully developed zone the pitot pressure is lower for the plain jet. Figure 3 shows the core length variation with NPR. It is interesting to note that, the co-flow is effective in increasing the supersonic core length of the primary jet at all NPRs ranging from 3-7, i.e. even in the presence of adverse pressure gradient. However, there is a negligible increment in the supersonic core length at NPR 8, for which the primary jet is almost correctly expanded. The maximum increase in the core length is for NPR 4 and it is negligible at correct expansion. Furthermore, the difference in the amplitudes of the pitot pressure oscillations between without and with co-flow reduces as the overexpansion level is decreased.

3.2 Shock structure and jet development

To study the jet development of both with co-flow and without co-flow, pitot pressure measurements in the radial direction at different axial locations were taken. The non-dimensionalised pitot pressure (P_t/P_0) is plotted against the radial distance (R/D), for both with and without co-flow cases at all the levels of overexpansion. Pitot pressure profiles in the near field are needed to quantitatively assess the shock structure and the far-field profiles for the jet development. The pitot pressure profiles are presented in Fig. 4. It is evident from these figures that, the pitot profiles are distinctly different for with and without co-flow cases. This implies that the shock structure and jet development are significantly influenced by the presence of co-flow. The measured pitot pressure (P_t/P_0) is the total pressure after the bow shock standing in front of the pitot probe. Hence, in the supersonic core region, a lower value of (P_t/P_0) indicates that the strength of bow shock is higher and the Mach number ahead of the bow shock is higher. After the supersonic core region, the decrease in (P_t/P_0) reflects mixing with the surrounding which leads to a decrease in velocity. As the probe traverses in the radial direction, the near-field value of (P_t/P_0) oscillates up to some X/D locations representing the extent of supersonic core.

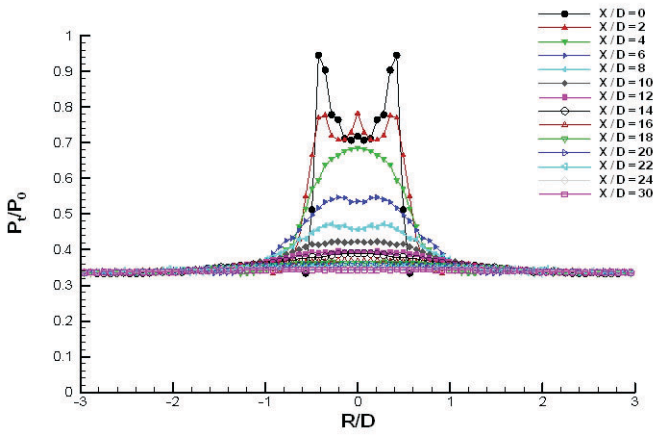
For NPR 3.0 the radial pitot pressure profiles are shown in Fig. 4(a) for without co-flow. From the radial pitot profiles, it is clear that the supersonic core extends up to about X/D = 4, as seen from small pressure oscillations. Downstream of X/D = 4, the pressure gradually decays at far-field up to X/D = 10. At further downstream locations the jet velocity becomes insignificant and no significant variation in pressure profile is observed. Off-centre peaks are seen at the exit of the nozzle due to interaction of bow shock ahead of probe with the nozzle exit flow. With co-flow (Fig. 4b) the pressure oscillations are seen up to X/D = 6. This implies that, due to the effect of co-flow the core is elongated and the jet far-field is also modified, as seen as insignificant variation of pitot pressure up to X/D = 16. For NPR 3, the pitot pressure at the co-flow nozzle exit is 42% of nozzle inlet pressure. The reason for this severe loss of total pressure experienced by the co-flow is two fold. The first and major cause for the pressure loss is that at the entrance of the co-flow passage, the passage is fed through 30 holes of 2·5mm diameter. Thus, there are 30 individual jets discharged into the co-flow passage. These jets severely interact before flowing as uniform flow up to the small parallel passage just downstream of the entry of the nozzle as illustrated in Fig. 1. This process essentially being a mixing process is bound to result in significant loss of total pressure. The second cause of pressure loss is the friction encountered by the co-flow due to outer surface area of primary nozzle and inner surface area of outer nozzle (co-flow passage). Hence, pressure ratio (P_t/P_0) calculated for the co-flow field is 1·35. Thus, the co-flow surrounding main jet flow is subsonic.

For NPR 4.0, the radial pitot pressure profiles are shown in Figs 4(c) and 4(d) for with and without co-flow, respectively. For without co-flow, the pressure oscillations are observed up to X/D = 4 and the pressure variation in the radial direction is significant up to X/D = 10. The pressure drop at the centre is more than that at NPR 3. With co-flow, the core extends up to X/D = 8 and the far-field pressure variations are observed up to X/D = 18. Hence, the co-flow not only modifies the near-field supersonic core, but also protects the far-field jet mixing significantly. The secondary flow starts interacting with the primary jet just after the exit and merges completely with primary jet at X/D = 6, as the radial extent of co-flow jet profile matches with primary jet for this axial location. The pressure ratio (P_t/P_0) calculated for outer co-flow is 1.60 for NPR 4, hence, the co-flow is high subsonic.

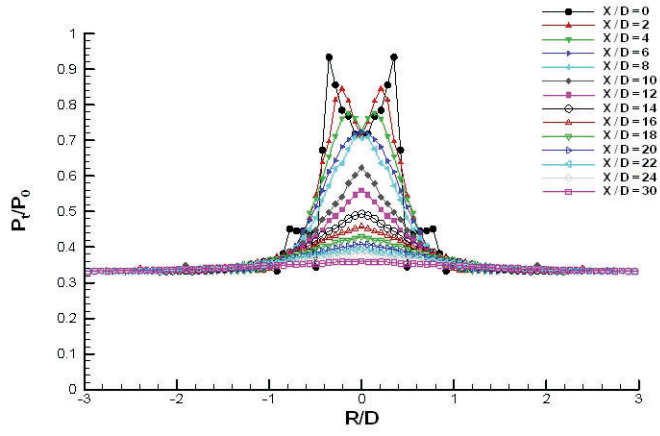
The radial pitot pressure profiles at NPR 5 are shown in Figs 4(e) and 4(f). When there is no co-flow, the pressure oscillations in the near-field extends up to X/D = 8, and in the far-field significantly reduced decay of pressure is observed up to X/D = 12. At X/D = 2, the pitot pressure profile exhibits a shock cross-over point. The centreline pitot pressure value is the lowest for this point and then the pitot pressure increases and again decreases as the probe traversing in the radial direction. The pitot pressure increases and drops toward the atmosphere pressure, as the probe is traversed outside the jet field. At X/D = 4, the pitot pressure around the jet axis is higher, as the probe is probably in the second shock cell, and downstream of the cross-over point such that, it traverses in the low velocity region. With co-flow, considerable pressure oscillations are observed up to X/D = 12, and as far as X/D = 24, the jet continues to posses significant momentum. The co-flow merges completely with the primary jet at about X/D = 10. The pressure ratio (P_t/P_0) calculated for the co-flow is 2·1, hence, the co-flow is underexpanded sonic jet with expansion level P_e/P_a = 1.11.

The radial pitot pressure profiles at NPR 6.0 are shown in Figs 4(g) and 4(h) for without co-flow and with co-flow, respectively. Pitot pressure oscillations are observed up to X/D = 8 and the

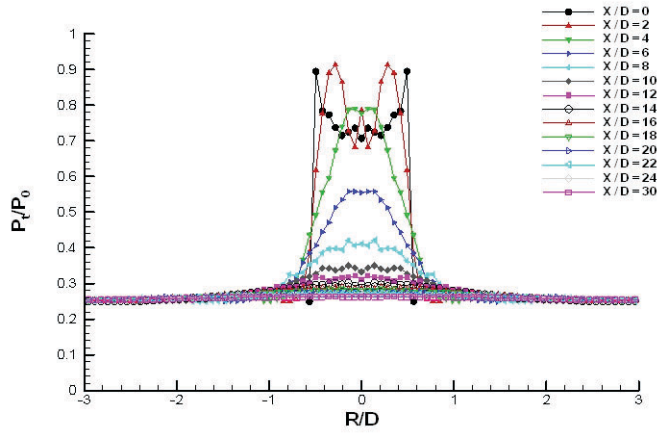
https://doi.org/10.1017/S0001924000002499 Published online by Cambridge University Press



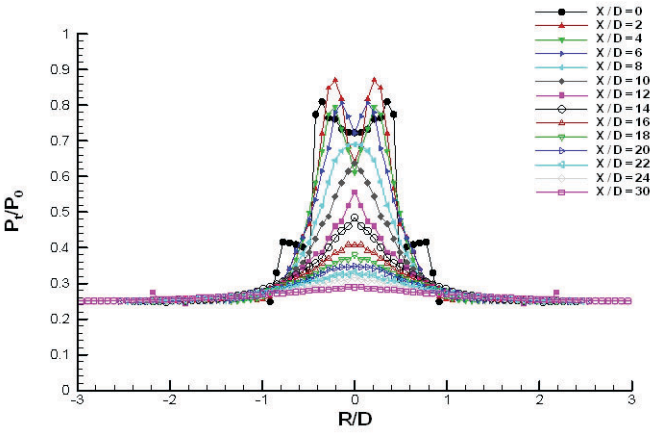
4(a) Without co-flow, NPR 3



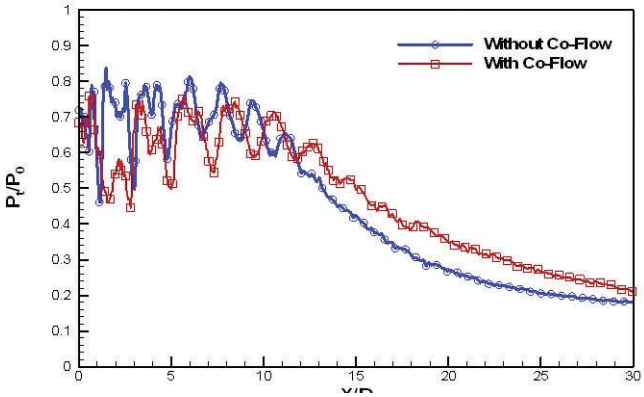
4(b) With co-flow, NPR 3



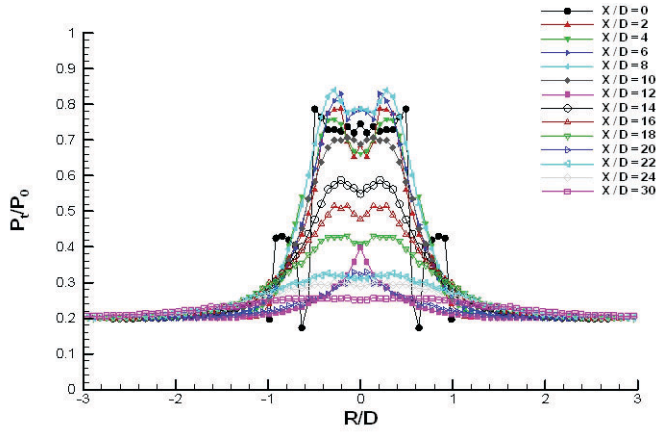
(c) Without co-flow, NPR 4



4(d) With co-flow, NPR 4



4(e) Without co-flow, NPR 5



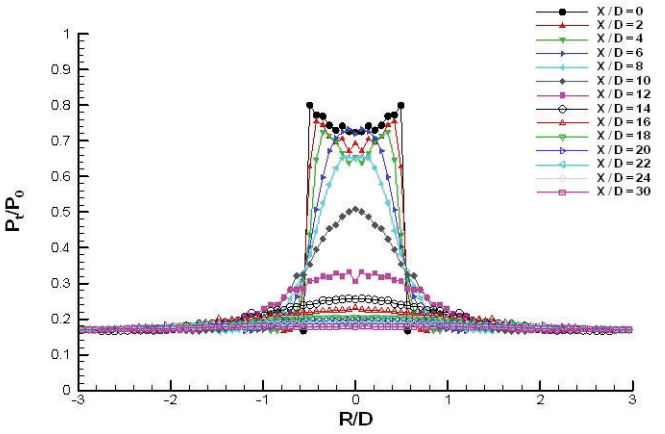
4(f). With co-flow, NPR 5

Figure 4 (a-f). Pitot pressure profiles in the radial direction.

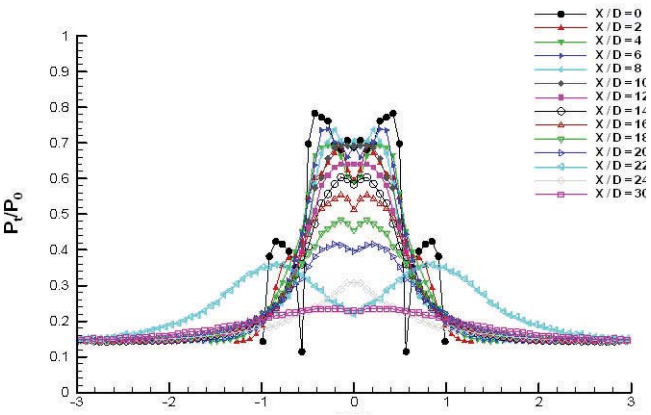
pressure variation in the radial direction is significant up to X/D = 14. In the near-field, shock cells become progressively smaller in size (radial extent) with increase of X/D. With co-flow, the pressure oscillations are seen up to X/D = 14, and the jet velocity remains significant up to X/D = 30. The pressure at the centre is lower than that without co-flow. Hence, the shock structure is significantly modified in the presence of co-flow. The secondary flow merges with the primary jet at X/D = 6. The expansion level for the secondary flow is 1·33 implying that the co-flow is underexpanded sonic jet.

The radial pitot pressure profiles for NPR 7 are shown in Figs. 4(i) and 4(j). The supersonic core extends up to X/D = 12 for without co-flow and the jet prevails up to X/D = 22. From the pitot profiles, it is observed that the mixing is moderately delayed. With co-flow, the supersonic core extends up to X/D = 14 and the jet prevails even beyond X/D = 30. The trend of pitot pressure profiles at NPR 6 and 7 are similar. The secondary jet merges with the primary jet at X/D = 8. The expansion level for the co-flow is 1·48, implying that the co-flow is underexpanded sonic jet. The radial pitot pressure profiles for

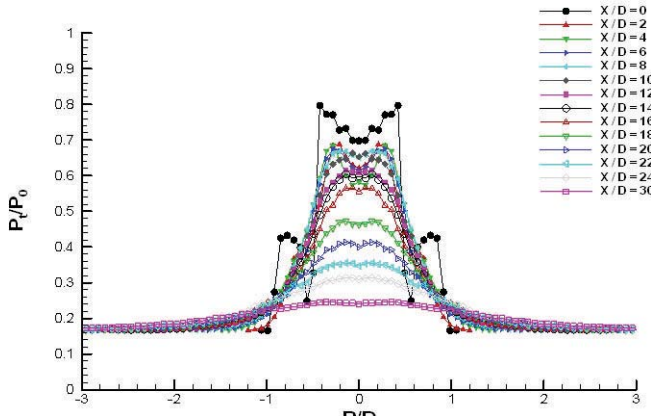
https://doi.org/10.1017/S0001924000002499 Published online by Cambridge University Press



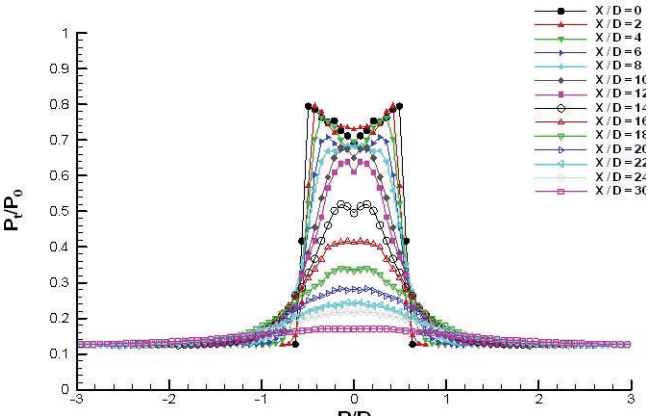
4(g) Without co-flow, NPR 6



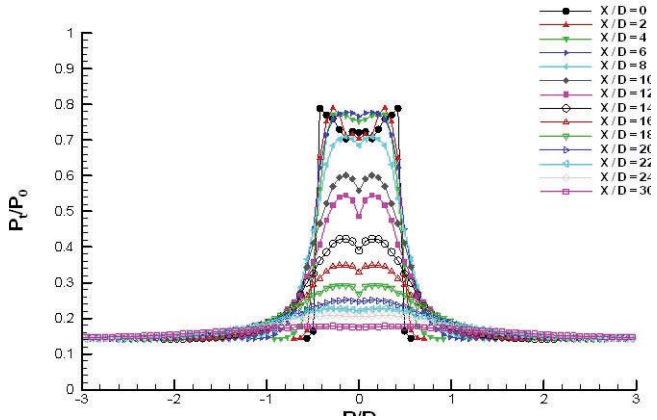
4(j) With co-flow, NPR 7



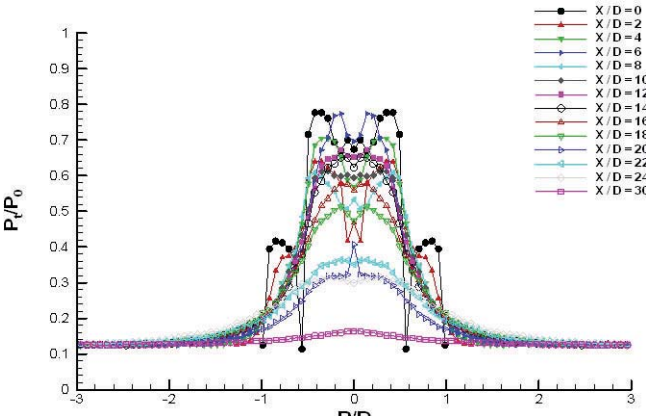
4(h) With co-flow, NPR 6



4(k) Without co-flow, NPR 8



4(i) Without co-flow, NPR 7



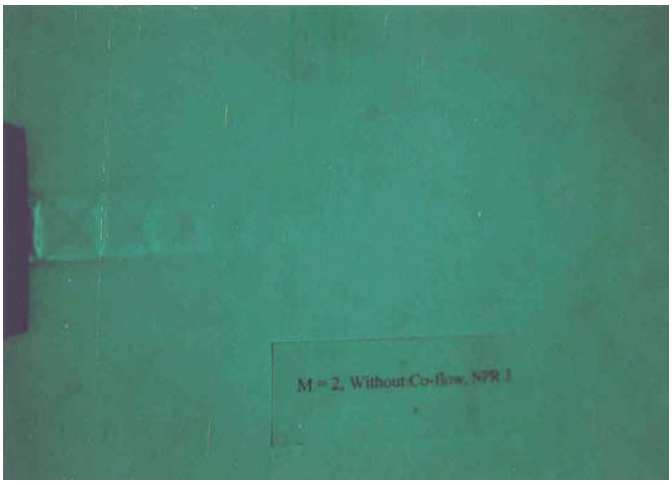
4(l) With co-flow, NPR 8

Figure 4 (g-l). Pitot pressure profiles in the radial direction.

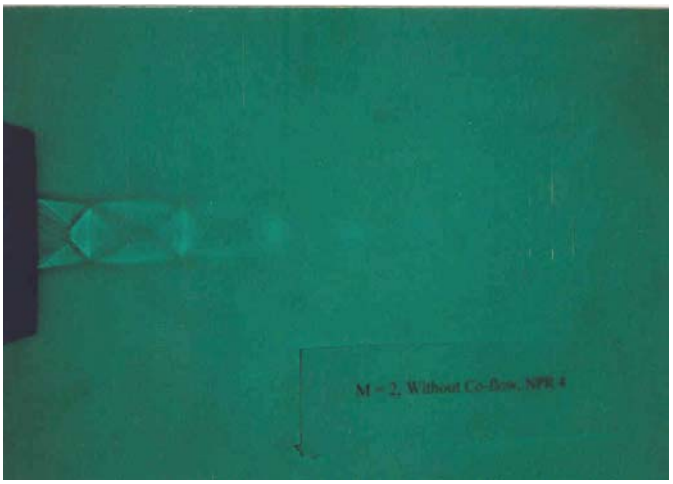
NPR 8 are shown in Fig. 4(k) for without co-flow and in Fig. 4(l) for with co-flow. NPR 8 is approximately correctly expanded state for Mach 2 jet. The supersonic core extends up to X/D = 14, for without co-flow. The far-field pressure variation is observed up to X/D = 30. With co-flow, the supersonic core extends up to X/D = 14. Hence, there is no supersonic core elongation for this NPR. The expansion level for the co-flow is 1·77. Hence, it may be stated that the interaction between the underexpanded co-flow and the correctly expanded primary flow from Mach 2 nozzle leads to no core elongation. The far-field pressure is higher than that for without co-flow case exhibiting that the subsonic portion of the jet prevails for longer axial distance.

Thus, the basic modifications with the introduction of co-flow in the jet field are elongation of supersonic core and inhibition of mixing at all levels of overexpansion for Mach 2 nozzle. For correct expansion, the core elongation is not significant, but the shock structure is modified and in the far-field the mixing is inhibited when the co-flow nozzle delivers subsonic and underexpanded jets.

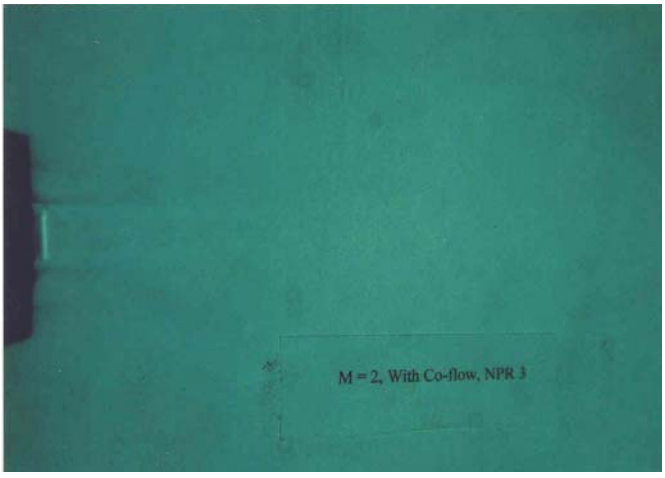
https://doi.org/10.1017/S0001924000002499 Published online by Cambridge University Press



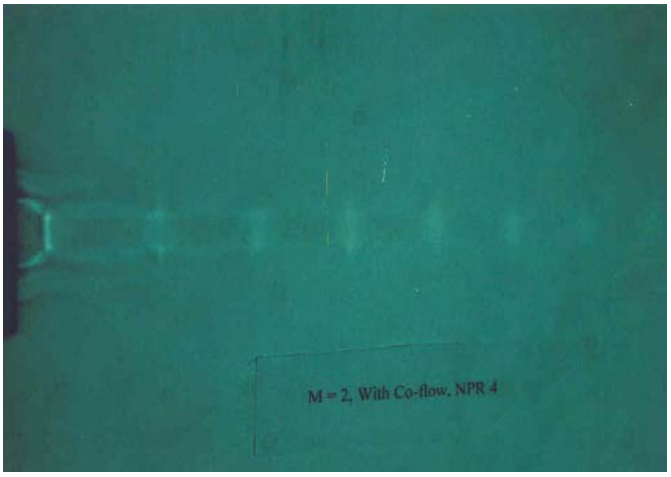
5(a) Without co-flow, NPR 3



5(c) Without co-flow, NPR 4



5(b) With co-flow, NPR 3



5(d) With co-flow, NPR 4

Figure 5 (a-d). Shadowgraph pictures at NPRs 3-8.

3.3 Flow visualisation

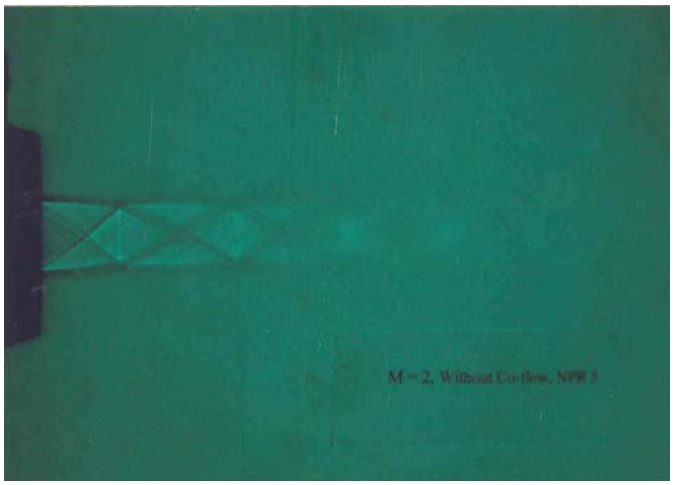
To study and visualise the jet structure grossly and at cellular level, shadowgraph pictures have been taken at different NPRs covering overexpansion and correct expansion level of Mach 2 nozzle, for both with and without co-flow. Radial pressure profiles can only give the pressure variation at coarse axial locations. Using shadowgraph internal shock-cell structure and the effect of co-flow presence can be visualized and explained qualitatively.

At NPR 3, the primary jet is overexpanded and the co-flow is subsonic. In overexpanded primary jet, the oblique shocks are formed at the nozzle exit and reflect as expansion fans from the free jet boundary. These expansion waves get reflected as compression waves from free jet boundary. This expansion and compression wave pattern forms shock cells, and this pattern repeats till the pressure in the supersonic core comes to an equilibrium with the surrounding atmosphere. In the first shock-cell the strength of oblique shocks and expansion waves are higher than the downstream shock cells. At this NPR for without co-flow (Fig. 5(a)), four shock cells are clearly seen in the shadowgraph picture. In presence of co-flow, the first shock-cell structure is changed as seen in Fig. 5(b). The secondary flow protects the primary jet from interacting with the still atmosphere and tries to penetrate into the primary jet. Hence, the primary jet boundary becomes curved, further downstream the shock cells are not clear in the shadowgraph. However, from the centreline pitot pressure distribution, it is clear that the primary jet core elongates in the presence of co-flow.

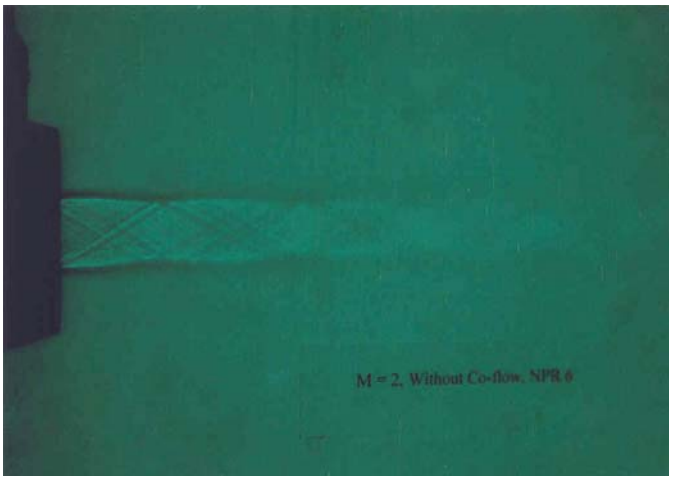
The shadowgraph pictures for NPR 4 are shown in Figs. 5(c) and 5(d), without and with co-flow, respectively. At this NPR also, the primary jet is overexpanded and the secondary flow is high subsonic. Without co-flow, four shock-cells are clearly seen and in the first shock-cell Mach disk is present. In the presence of co-flow, the Mach disk becomes wider in the first shock-cell as the oblique shocks as well as the primary jet boundary become curved. The first shock-cell length reduces but the lengths of the downstream shock cells increase. The number of shock cells increased to seven.

The shadowgraph pictures for NPR 5 are shown in Figs 5(e) and 5(f) for without and with co-flow, respectively. At this NPR the primary jet is overexpanded and the co-flow jet is underexpanded sonic jet with an expansion level of 1·11. In without co-flow case, diamond shock-cell pattern is seen and the number of shock cells is five. With co-flow, a small Mach disk is formed in the first shock-cell and the axial extent of first shock-cell reduces. The oblique shock at the nozzle exit curves towards the centreline. A mild penetration of the reflected oblique shock in the surrounding flow is seen. The downstream shock cells increase in length and the number of shock cells is six in the presence of co-flow. At NPR 6 also (Figs. 5(g) and 5(h)), the primary jet is overexpanded and the co-flow is

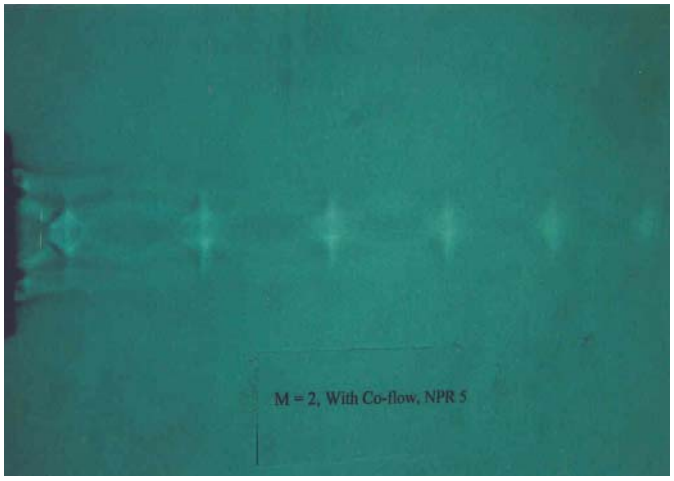
https://doi.org/10.1017/S0001924000002499 Published online by Cambridge University Press



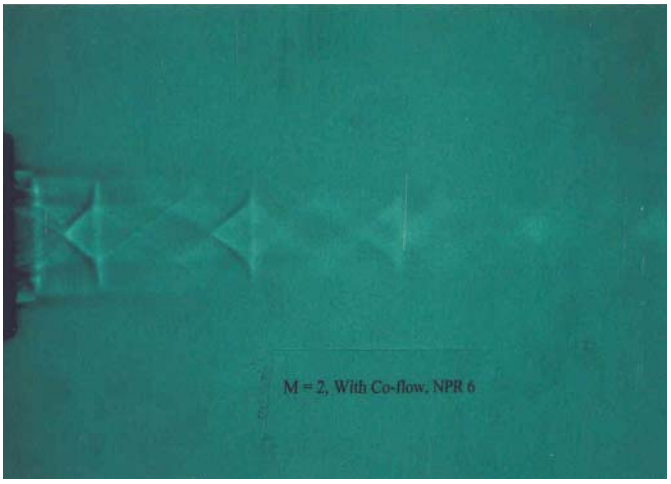
(e) Without co-flow, NPR 5



5(g) Without co-flow, NPR 6



5(f) With co-flow, NPR 5



5(h) With co-flow, NPR 6

Figure 5 (e-h). Shadowgraph pictures at NPRs 3-8.

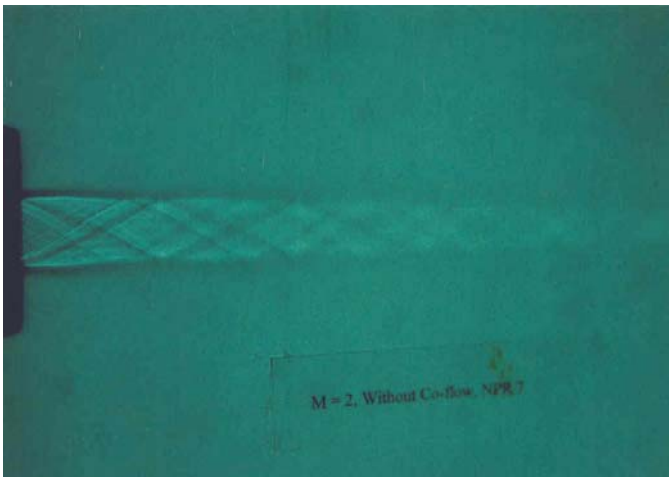
underexpanded sonic jet with an underexpansion level of 1·33. When there is no co-flow, as the overexpansion level comes down, the strength of the oblique shock decreases as is seen in Fig. 5(g). In the presence of co-flow, the oblique shocks at the exit get deflected toward the jet centreline from the point of interaction of the underexpanded co-flow with the primary jet. No Mach disk is formed for this case, because the oblique shocks become stronger than without co-flow case and give rise to the stronger compression accordingly. The reflected shocks become curved and penetrate into the underexpanded surrounding flow. Due to the merging of the two jets, there is an increase in the size of the downstream shock-cells. At NPR 7 (Figs 5(i) and 5(j)), the primary jet is mildly overexpanded and the co-flow is underexpanded with an underexpansion level of 1·48. When there is no co-flow, the trend is similar to NPR 6. With co-flow also the trend is similar to NPR 6, but the downstream shock-cell lengths are increased whereas the shock strength has decreased. The reflected shock is weaker and more curved outwards. NPR 8 (Figs 5(k) and 5(l)) is close to correct expansion for the primary jet, whereas the co-flow underexpansion level is 1·77. For without co-flow, there is no significant pressure imbalance for the exiting flow, but the flow has a larger space to relax. Because of this expansion fans formed at the nozzle lip. These expansion waves reflect as compression waves from the free jet boundary and form shock-cell. With co-flow, the deflection of the reflected shock is still less pronounced. The strength of the shocks decreases and the number of shock-cells increases. But, no elongation in supersonic core is observed. The penetration of shock waves in the outer flow at higher NPRs suggests that there is not much of a boundary between the primary flow and the co-flow, i.e. they are of similar speed. But there are some complex flow physics happening here that need further study and higher quality measurements, focusing mainly at the boundary between the two flows, to better understand the flow process.

In all the overexpanded cases studied, the number of shock-cells increases with co-flow. For overexpanded primary jet in subsonic co-flow, the Mach disk formation is observed and the Mach disk size is decreased when the co-flow becomes underexpanded. For higher underexpansion level of co-flow, Mach disk is not formed.

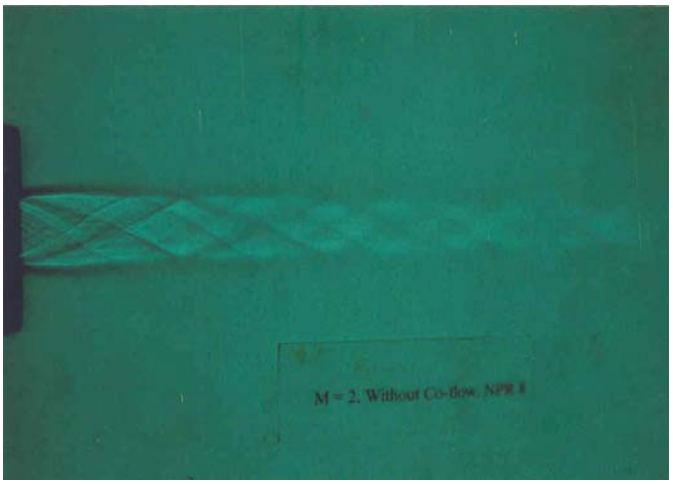
4.0 CONCLUSIONS

Co-flow significantly modifies the primary jet characteristics, influencing the shock-cell structure and far-field mixing activity. Presence of co-flow retards mixing and hence, acts as mixing inhibitor at all levels of overexpansion. The primary jet encounters a moving boundary when an annular flow is introduced which elongates the core length by a maximum of 104% at NPR 4. The supersonic core length increases significantly at all NPRs of the overexpanded flow regime. Negligible core elongation is observed

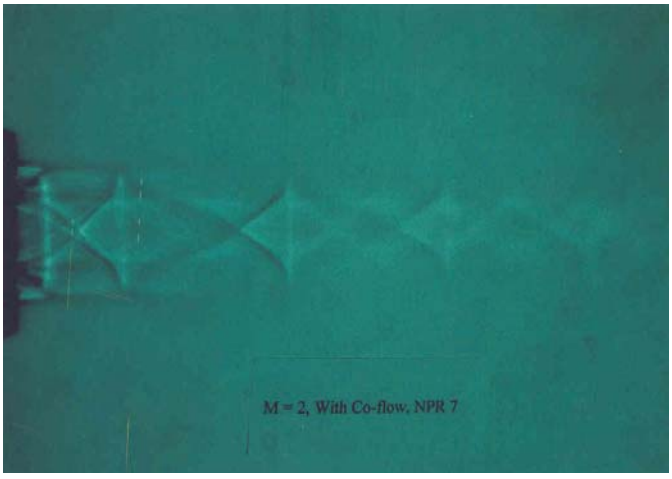
https://doi.org/10.1017/S0001924000002499 Published online by Cambridge University Press



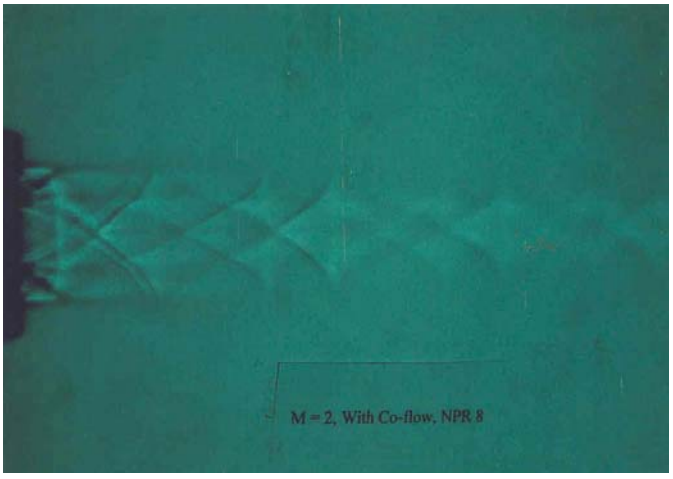
5(i) Without co-flow, NPR 7



5(k) Without co-flow, NPR 8



5(j) With co-flow, NPR 7



5(l) With co-flow, NPR 8

Figure 5 (i-l). Shadowgraph pictures at NPRs 3-8.

for approximately correctly expanded primary jet in the presence of underexpanded co-flow. By the introduction of co-flow, the first shock-cell length of the primary jet is reduced and there is a significant increase in the number of shock-cells. For Mach 2 overexpanded primary jet, in the presence of subsonic co-flow, the Mach disk formation is observed and the Mach disk size decreases when the co-flow becomes underexpanded.

REFERENCES

1. PAPAMOSCHOU, D. and DEBIASI, M. Noise measurements in supersonic jets treated with the Mach wave elimination method, *AIAA J*, 1999, **37**, (2), pp 154-160.
2. PAPAMOSCHOU, D. Mach wave elimination in supersonic jets, *AIAA J*, October 1997, pp 1604-1611.
3. DEBIASI, M. and PAPAMOSCHOU, D. Noise from imperfectly expanded supersonic coaxial jets, *AIAA J*, March 2001, pp 388-395.
4. MURAKAMI, E. and PAPAMOSCHOU, D. Mixing layer characteristics of coaxial supersonic jets, 1986, AIAA paper 86-0162.
5. SUKUMAR, V.N., SUNDARAVADIVELU, T., LOVARAJU, P. and RATHAKRISHNAN, E. Effect of co-flow on near field shock structure of underexpanded central jet, 2007, Ninth Asian symposium on visualization, ASV0031-001.
6. SUNDARAVADIVELU, T., SUKUMAR, V.N., LOVARAJU, P. and RATHAKRISHNAN E. Experimental studies of co-flowing jets for mixing inhibition, 2007, AIAA paper 4497.
7. LOVARAJU P., CLEMENT, S. and RATHAKRISHNAN E. Effect of cross-wire and tabs on sonic jet structure, *Shock Waves*, 2007, **17**, pp 81-83.

https://doi.org/10.1017/S0001924000002499 Published online by Cambridge University Press